A new approach to three-dimensional intermesh clearance calculation

D Richter, H Müller
TU Dortmund, Department of Computer Science VII, Germany
K Nadler, A Brümmer
TU Dortmund, Chair of Fluidics, Germany

ABSTRACT

A novel approach to three-dimensional inter-surface clearance calculation for twin-shaft rotary displacement machines based on a NURBS representation of both rotor surfaces is presented. The calculation is split up in separate steps. At first, a tree data structure of both surfaces is created by using bounding volumes. Based on the tree structure, an efficient identification of nearest pairs of bounding volumes is possible. In the next step, a contour line with a fixed, user defined distance is created with the marching squares algorithm. The contour line encloses a stripe-shaped region which is triangulated by means of dynamic programming so that the total length of the triangle edges is minimized. For each edge, a closest point on the opposite surface is calculated with the Newton algorithm. The resulting intermesh clearance is represented by the resulting set of closest points. A comparison with of the approach to other common methods shows several advantages. The use of NURBS surfaces guarantees a good mathematical accuracy for miscellaneous rotor profiles as well as the possibility to communicate directly with common CAD-systems. Finally the new approach for the intermesh clearance calculation is compared to another calculation method and the advantages and improvements are shown.

SYMBOLS

Symbol	Unit	Meaning
a_i	[-]	point of the first component of the iso-distance line
$B(i,j)$	[-]	weight of a path of minimum weight to the node h_{ij}
b_i	[-]	point of the second component of the iso-distance line
e	[-]	number of points of the first component of the iso-distance line
f	[-]	number of points of the second component of the iso-distance line
$f_{ij}(x)$	[-]	parameters (u,v) at parameter x along triangulation edge t_{ij}
H	[-]	grid graph for triangulation
h_{ij}	[-]	grid node at index i and j of grid graph H
L_1	[-]	list of points of the first component of the iso-distance line
L_2	[-]	list of points of the second component of the iso-distance line
l_{ij}	[-]	length of a triangulation edge t_{ij}
m	[-]	number of control points in u-direction
$N_{i,p}$	[-]	B-spline basis function evaluated at i for degree p
$N_{j,q}$	[-]	B-spline basis function evaluated at j for degree q
n	[-]	number of control points in v-direction
P	[-]	control polygon mesh
p	[-]	degree of NURBS-surface in u-direction
P_{ij}	[-]	control point with indices i and j

$P_{x,t_{ij}}$	[-]	point of the NURBS-surface evaluated at parameter x along edge t_{ij}
q	[-]	degree of NURBS-surface in v-direction
$R_{i,j}$	[-]	rational base function evaluated at i and j
r	[-]	size of U (knot vector)
S (u,v)	[-]	NURBS-surface function evaluated at (u,v)
s	[-]	size of V (knot vector)
$t_{i,j}$	[-]	triangulation edge between the points a_i and b_j
U	[-]	knot vector in u-direction
u	[-]	knot of U knot vector
V	[-]	knot vector in v-direction
v	[-]	knot of V knot vector
W	[-]	weight matrix
$W_{i,j}$	[-]	weight with indices i and j

1 INTRODUCTION

Fluid energy machines in positive displacement design play a great role in a number of technical applications. Here, the twin-shaft rotary displacement machines, which due to the purely rotary movement and the simple and rugged design have decisive advantages compared to the oscillating designs. The typical field of application of the twin-shaft rotary displacement machine as compressor comprises e.g. the automobile sector, cooling systems, compressed-air generation, chemical process plants as well as the vacuum technology. The twin-shaft rotary displacement machine is also used as a motor. Here, it is often applied in systems with small and medium output in Clausius-Rankine-processes. Apart from the field of application, another classification criterion is the differentiation between wet- and dry-running designs. However, the contamination of the working fluid with coolants or lubricants, as they are used in wet-running machines, is not acceptable in all fields of application, thus there is a clear trend towards dry-running machines.

Although the fields of application are very diverse, there are also commonalities of all rotary displacement machines with regard to geometry, construction and their basic thermodynamic and fluid-mechanical operating behaviour. One of the features is the function-related clearance between the static and the rotating components as well as between the rotating components, which gain importance due to the mentioned renunciation of coolants and lubricants. The clearance geometry as a part of the total geometry is to be determined by the design and has a decisive impact on the operating behaviour and thus on the integral parameters, as for example the volumentric efficiency. In this context, the clearance heights are always a compromise between operating safety and the quality of energy conversion. The clearance height design in cold undeformed state requires basic knowledge about the thermal and mechanical load occuring in operation and the deformations and shifting at components and bearings. However, this information needs to be geometrically evaluable in order to enable the determination of the clearance heights in operating condition. Although for typical rotary displacement machines there are different types of clearances, the focus of the following explanations is on the intermesh clearance, since from the geometric point of view this is the most complex case.

For the definition of the intermesh clearance, a difference can be made between two terms: the line of contact or line of action and the quasi-line of action. The line of contact only exists for a geometrically ideal profile, which is calculated e.g. by means of the law of gearing. It represents the connecting line of all points, in which the rotor flanks roll off against each other. For an arbitrary executable profile with existing profile clearance height, however only a quasi-line of action exists. From the geometry point of view, it can be defined by the minimum distance of the two rotor surfaces from each other.

2 STATE OF THE ART

Analogously to the definition of the term, there are two principle approaches conceivable for the calculation of the line of action. One possibility is the application of a toothing method; the other is the geometric calculation of lines of minimal distance of the rotor surfaces.

The application of the involute method or cycloidal method enables the caclulation of the ideal profile of the female rotor. The related line of action is implicitly included in the calculation, since the toothing method determines all pitch points. Possible methods for the calculation of the female rotor profile, which is free of play, are to be found e.g. in (1) and (2). In principle, also the reversal of this method is conceivable, in which the related female rotor is calculated on the basis of the desired line of action. This approach is described e.g. by (3) and (4). Although the calculation of the female rotor is usually only used for the two-dimensional rotor profile, the three-dimensional extent of the line of action can be calculated with the help of length and wrap angle of the male rotor.

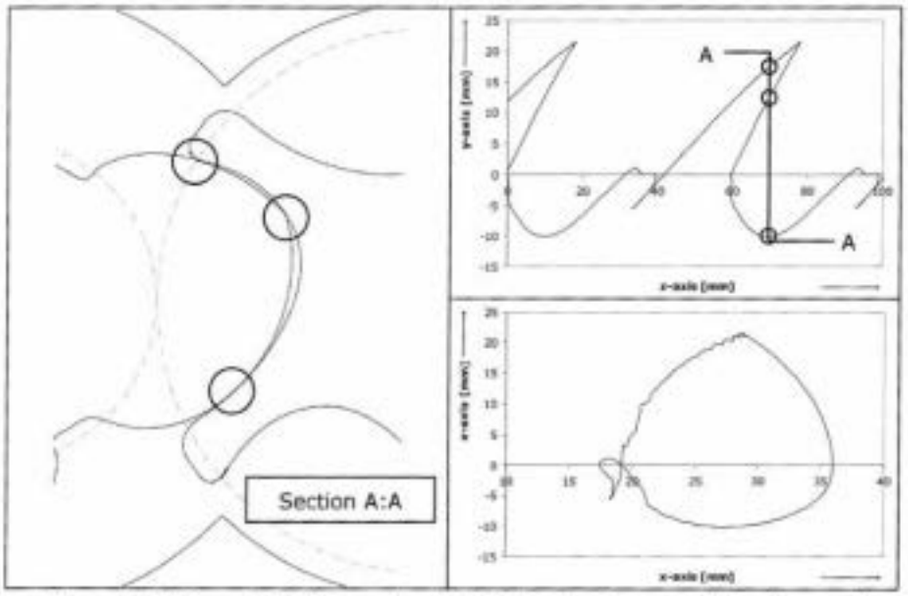

Figure 1: Undercut in the quasi contact line in rotor axis direction and influence on two-dimensional calculation approaches

The effective geometric calculation of the quasi-line of action is a demanding task, since the rotor surfaces can be arbitrarily shaped. Based on a geometric representation of the surfaces, the amount of point pairs of the minimal distance can be searched with the help of different heuristics and be combined to a line on each rotor surface. Here, a difference can be made between two and three-dimensional approaches. For the two-dimensional approaches, a simplification is carried out to the effect that they transfer the search for minimal distances to the transverse section of the rotor. This reduces the geometric complexity considerably, since only minimal distances between two arbitrary designed rotor contours need to be calculated. This limitation however results in possible complications in regions in which the quasi-line of contact shows an undercut in rotor axis direction. In these areas, there is no clear solution concerning the minimal distances of the rotor transverse sections so that an evaluation of the minimal distances is required (**Figure 1 Section A-A**). Such a method is presented in (5) and (6). Alternatively,

the analysis can be carried out completely three-dimensionally. This kind of method is presented in (7).

The decisive characteristic of this method is the iterative approach. Based on the analysis of both rotor front sections, two suitable starting points for the actual calculation are determined. Starting from these points, an initial quasi-line of contact is formed, which in a first step connects only these two points directly and thus only corresponds to an extreme approximation of the quasi-line of contact. In the following, this line will be further refined according to the bisection method (**Figure 2**). For this purpose, a line between two known points is drawn perpendicularly to the previous course of the quasi-line of action towards the surface of one of the rotors. Based on this line, the point of minimal distance to the counter rotor surface is determined and included into the amount of the previously calculated quasi-points of contact (Figure 2). This procedure will be repeated until sufficient approximation of the line of action has been achieved.

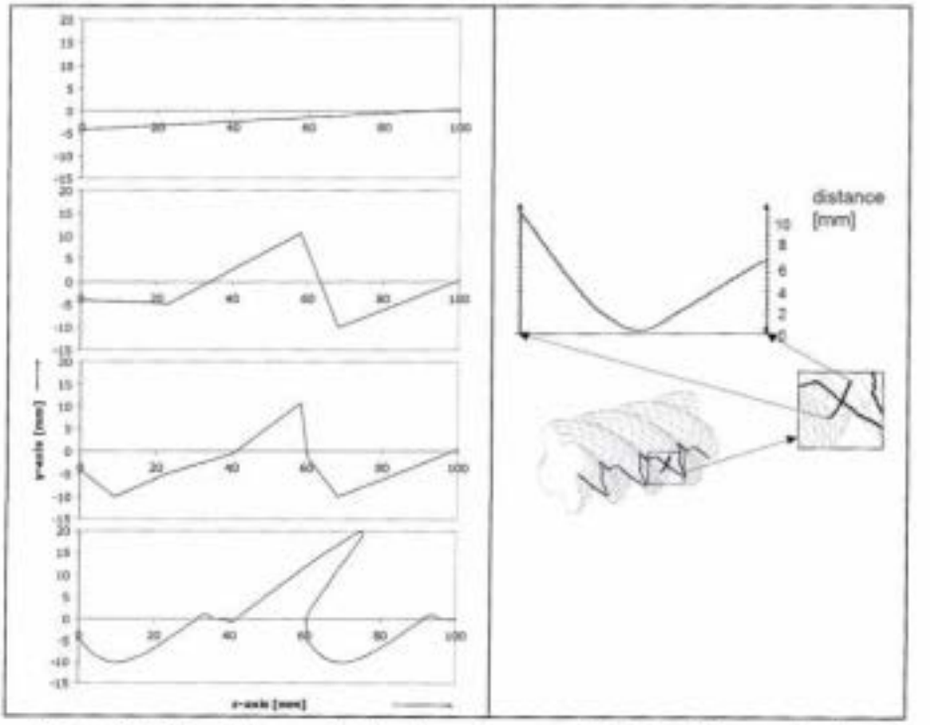

Figure 2: Calculation and inclusion of a new point of action acc. to the bisection method

Both principles for the calculation of the line of action resp. quasi-line of action bear both advantages and disadvantages. The advantages of the calculation based on the toothing method are the low computational effort and the often analytical approaches which can be transferred to a number of geometric representations. A disadvantage is the fact that only the geometric course of the line of action is calculated and thus the clearance height becomes zero, explicitly in all contact points. Accordingly, the application to thermally/mechanically deformed profiles or those with clearance is only conceivable as an approximate solution. Moreover, e.g. the law of gearing is not respected in case of all technically relevant rotor profiles so that here, too, the limited variety of applications needs to be accepted.

The advantage of geometric methods is their principally universal validity. The only prerequisite is the rotor geometry being able to be reflected with sufficient accuracy in the geometric representation required by the method. This also allows the analysis, e.g. of thermally/mechanically deformed geometries. A decisive disadvantage is the clearly higher computational effort, since there are no exact resp. analytical solutions available for such complex free-formed surfaces. According to the approach, the quality of the result strongly depends on the quality of geometric representation and search strategy. Here, usually information on maximum and minimum intermesh clearance height is of avail.

The calculations require a geometric representation of the rotor surfaces as a basis, which is provided by the user. In contrast to other methods (e.g. (7), the representation is not point-based, but uses parametric NURBS-surfaces.

3 SURFACE REPRESENTATION OF ROTORS USING NURBS

NURBS (Non Uniform Rational B-Splines) are frequently used in graphical data processing. The advantages are the intuitive geometric feature, the numerical stability and the efficient calculation. Many CAD-systems use NURBS for the representation of surfaces and curves so that in this system, rotor surfaces can be manipulated and processed.

NURBS are bivariate tensor points plotting R^2 against R^3. The definition of a NURBS surface with a degree (p,q) consists of the following components:

A control polygon mesh P with n x m knots

$$P = \{P_{i,j} \in R^3,\ i = 0,\dots,n-1,\ j = 0,\dots,m-1\} \qquad \text{Eq. 1.}$$

the knot vectors U and V, with

$$U = \{\underbrace{0,\dots,0}_{p+1}, u_{p+2},\dots,u_{r-p-1}, \underbrace{1,\dots,1}_{p+1}\} \qquad \text{Eq. 2.}$$

$$V = \{\underbrace{0,\dots,0}_{q+1}, v_{q+2},\dots,v_{s-q-1}, \underbrace{1,\dots,1}_{q+1}\} \qquad \text{Eq. 3.}$$

in which the length of the knot vectors r and s is

$$r = n + p + 1 \qquad \text{Eq. 4.}$$

$$s = n + q + 1 \qquad \text{Eq. 5.}$$

and the weight matrix W

$$W = \{W_{i,j} \in R^1,\ i = 0,\dots,n-1,\ j = 0,\dots,m-1\} \qquad \text{Eq. 6.}$$

The parametric function of the NURBS-surface S is defined as

$$S(u,v) = \sum_{i=0}^{n-1}\sum_{j=0}^{m-1} R_{i,j}(u,v) \cdot P_{i,j} \qquad \text{Eq. 7.}$$

in which $R_{i,j}$ is the rational base function

$$R_{i,j} = \frac{N_{i,p}(u) \cdot N_{j,q}(v) \cdot W_{i,j}}{\sum_{k=0}^{n-1}\sum_{l=0}^{m-1} N_{k,p}(u) \cdot N_{l,q}(v) \cdot W_{k,l}} \qquad \text{Eq. 8.}$$

In this, N is the B-spline base function related to degree p and q based on the knot vectors U and V.

Thus the function S is piecewise composed of rational functions. If a control point or a weight changes, the impacts of this change are only locally observed. This is in contrast to the basic principle of the Bézier-surfaces, on which changes have a global effect (8).

For the modeling of the rotor, only the peripheral surface is calculated. The front sides are not included in the model, since they are not required for the calculation of the intermesh clearance. Furthermore, volume rendering is not applied, as only the surface of the rotor has to be used for the distance calculation.

In most cases, the rotor geometries examined are given as a set of points. These sets of points must now be transferred into NURBS-surfaces, for which basically different methods exist. Some works, as for example (8), describe an approximation of the NURBS-surfaces with the help of least squares, (10) presents an evolutionary calculation approach and (11) describes an algorithm for the interpolation of the surfaces. Which of the approaches is followed often depends on the actual application. **Figure 3, left,** shows an exemplary calculation of a surface acc. to (11).

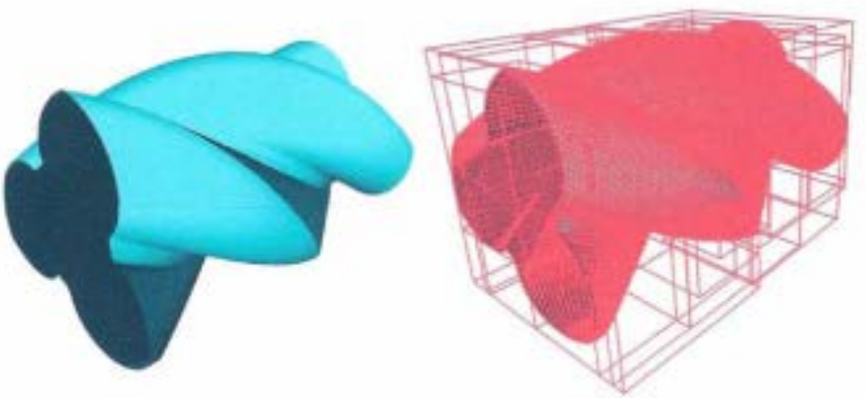

calculated rotor surface bounding volumes

Figure 3: Surface of the male rotor GI 51.2 (9) and the related bounding volume hierarchy with Axis Alligned Boxes (AAB) in the depth increments 1, 2, 3 and 7

4 CALCULATION OF THE LINE OF ACTION

In the following, an approach to the geometrical calculation of the quasi-line of action is presented which is based on a NURBS-representation of both rotor surfaces, with the calculation method being principally applicable to any parametric surface. The calculation of the quasi-line starts with an iterative subdivision of the parameter spaces of the two rotor surfaces, resulting in sub-surfaces which are organized in two tree structures. A collision test based on the bounding volumes of the finest sub-surfaces of the male and female rotor, which can be found on the lowest tree level, enables the identification of parameter sub-spaces in which the rotor surfaces have a minimal distance. In the next step, an equidistant grid is introduced in this parameter space of the rotor, the nodes of which are each in the centers of the squares determined before. Now, the minimal distance from each

point of the grid to the surface of the other rotor is calculated. Based on the Marching-Squares Algorithm and the predetermined maximum distance, the iso-distance line of this value is formed by a polygonal chain. The iso-distance line outlines a strip-type region in which the quasi-line of action will be searched. For this purpose, a method of dynamic programming is applied to two components of a iso-distance lines in the parameter space to obtain a triangulation with an overall minimal length of all triangulation edges. Now, the minimum distance between the two rotor surfaces can be calculated along such an edge.

4.1 Calculation of a Bounding Volume Hierarchy

A widespread approach in graphical data processing is the simplification of complex geometrical objects with the help of bounding volumes. (12) describes several procedures and kinds of bounding volume elements commonly applied in the bounding volume hierarchy. In this case, the bounding volume hierarchy is created by a quad tree subdivision in parameter space. A subdivision step consists mainly of the quartering of a square in parameter space into four equal squares by bisecting the boarder of the parent square. Then a bounding volume for the sub-surface of the rotor surface induced by every square in parameter space is calculated, which additionally envelopes the union of the bounding volumes of its sub-sub-surfaces. **Figure 3, right,** shows an example of a bounding volume hierarchy for the male rotor geometry.

4.2 Collision Test

Since the distance between the rotors of a rotary displacement machine is small compared to its outer dimensions and the rotors usually mesh like screws, it is possible to determine the regions on the rotor surfaces having the smallest distance. In this context, the bounding volume hierarchies of the two rotors calculated before are used.

(12) describes several approaches to test two bounding volume hierarchies for collision. In this work, the approach of simultaneous depth-first search is preferred, because in both hierarchies, subtrees which do not show collision fall away and thus considerably less calculation time is required (12). Since the bounding volume hierarchies of both rotors shall have the same structure, the levels of the quad tree can be tested for collision in pairs. Hence, it is started with the roots of both hierarchies. Only in case of a collision, the children of the collided bounding volumes are examined in the next level. If there is no collision, the sub-trees are discarded for further collision tests.

This procedure is repeated until collisions cease to occur or until the algorithm has reached the last level of the quad tree. Here, all bounding volume elements, together with those of the counter rotor, are now tested for collision and as a result, it is stored with which element of the other hierarchy a collision took place. The marking of the bounding volume elements can help in the further course of calculation, for example in the calculation of the initial values for the Newton's iteration.

4.3 Iso-Distance Lines

The collision test is the basis for the calculation of the iso-distance lines in the parameter space. Now, from the quadrants in the parameter space of the rotor, which belong to the lowest level of the quad tree, an equidistant grid is formed again in the parameter space, with the nodes of the grid being in the center of the quadrant. Initially, each grid node receives only one piece of digital information about the collision. The grid nodes with a collision attribute define a region in which a collision occurs or both surfaces are nearby (**Figure 4**). A polygonal chain of the outline can be calculated by means of the Marching-Squares Algorithm (13).

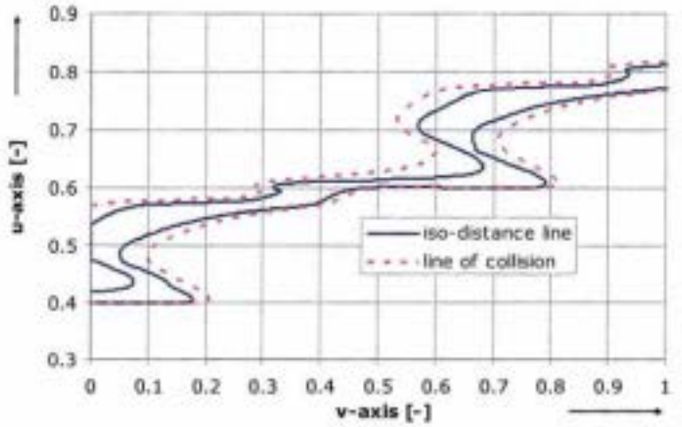

Figure 4: Results of the Marching-Squares Algorithm for the collision range and for a determined distance, shown in the parameter space of the female rotor

Compared to the whole parameter range of the female rotor surface, this range already represents a significant restriction; however there is still need for improvement, in particular in the region of the undercuts along the v-axis. An improvement can be achieved by predetermining a maximum distance. For this purpose, the distance to the other rotor surface is first calculated for all grid points with collision information and then compared to the predetermined maximum distance. The grid points with a distance lower than the maximum distance are labelled. An application of the Marching-Squares Algorithm to the resulting labelled grid with the predetermined maximum distance as iso-value is a region limited by the iso-distance line (Figure 4). This is again smaller than the region of the collisions and thus more suitable for the further processing. The iso-distance line, which can fall to pieces, is geometrically represented by a polygonal chain. Such a region is named as nearby-region in the following.

4.4 Triangulation

The calculation of the quasi-line of action is based on the following assumptions, which are feasible due to study of practical situations (**Figure 5a**).

1. The nearby-region is strip-type and is outlined by two components of the iso-distance line.
2. The quasi-line of action is almost parallel to both components of the iso-distance line.
3. For a connecting line segment of two nearby points on both components of iso-distance lines, there is only one point in parameter space whose corresponding surface point has a minimum distance to the other surface.

Now, the basic idea is to calculate, for a set of densely located connectig line segments along the nearby region, the corresponding surface points of minimum distance according to 3, and to report them as a representation of the quasi-line of action.

A simple approach to define the connection lines would be the selection of lines parallel to the vertical (v-axis) or horizontal (u-axis) direction. Figure 5b and c show that based on those connection lines the search for only one local minimum cannot be successful. Here, problems similar to those of the simplified three-dimensional methods are to be expected (5), (6). For this reason, the connection

lines must adapt themselves dynamically to the region, as is to be seen in Figure 5d. To reach this goal, a technique described in (14) is adopted. This method calculates for two given similar and closed polygonal chains in two parallel planes in space a ring-shaped connecting surface. The surface is then represented by a triangle mesh which is defined by selected edges between vertices of the upper and lower polygonal chain together with the edges on the polygonal chains. The quality of the triangle mesh can be specified by an objective function, like e.g. minimisation of the area of the calculated surface.

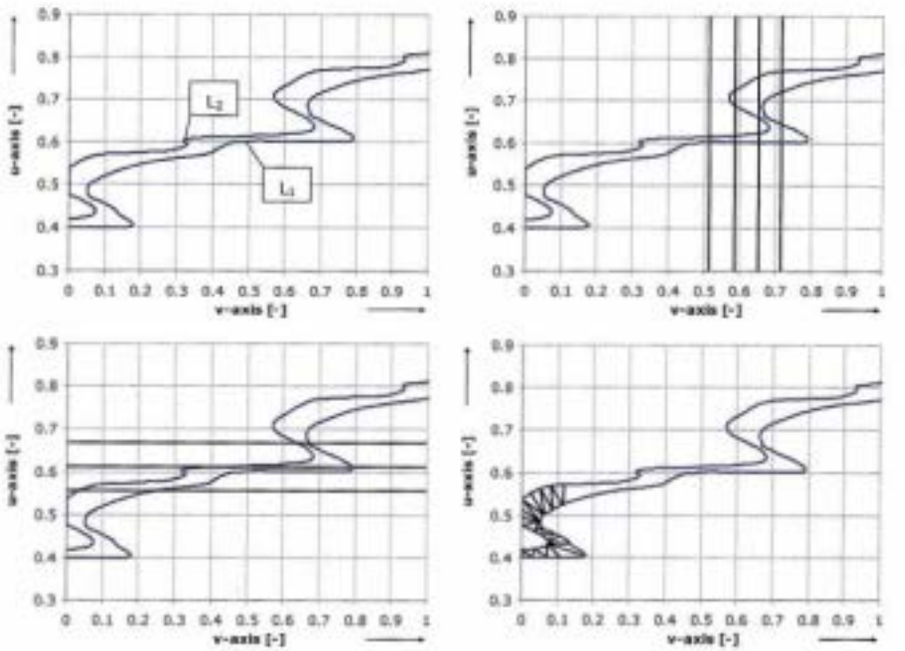

Figure 5a: typical form of the nearby-region
Figure 5b: static cutting of the region in u-direction
Figure 5c: static cutting of the region in v-direction
Figure 5d: dynamic cutting by means of triangulation edges

This method is now transferred to the given situation in that the two components of the iso-distance line are represented by two polygonal chains with densely located vertices. The polygonal chains are the two polygonal chains delivered by the Marching Squares Algorithm in the parameter space and bounding the nearby region. Between the two polygonal chains, a triangle mesh is determined which is induced by edges between the polygonal chains together with their edges. The objective is to minimize the sum of the lengths of the mesh edges between the chains, in order to achieve connections of nearby opposite points. Figure 5c illustrates a mesh of this kind.

Let

$$L_1 = \{a_0, a_1, \ldots, a_{s-1}\}, \quad a_i \in R^2 \text{ and}$$
$$L_2 = \{b_0, b_1, \ldots, b_{t-1}\}, \quad b_j \in R^2$$

denote the lists of vertices on the polygonal chains. In the following, a triangulation edge between the points a_i and b_j in the parameter range will be called $t_{i,j}$. In order to enable the calculation of all triangulation edges in the first step, the triangulation

edges to all points b_j of the second point list L_2 are calculated starting from each point a_i of the first list L_1. Here, the length $l_{i,j}$ of an edge $t_{i,j}$ is defined as Euclidean distance of the related points in the image domain.

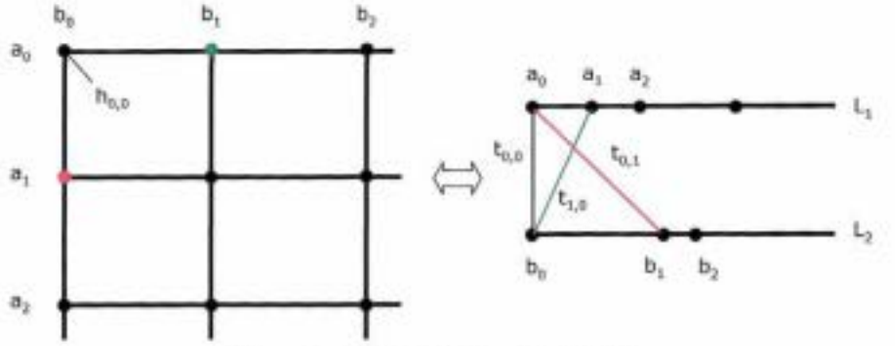

Figure 6a: Exemplary grid graph H
Figure 6b: Exemplary triangulation for e=f=3 between L_1 and L_2

The calculated edges and their lengths are organized in a grid graph (**Figure 6a**). The dimension of the grid graph is defined by the number of elements e and f of the two polygons L_1 and L_2. A node of the grid graph $h_{i,j}$ is weighted with the length $l_{i,j}$ of the related edge $t_{i,j}$.

An optimum triangulation between the two components L_1 and L_2 of the iso-distance line can now be determined as a monotone path through grid graph H, which minimizes the total sum B(e-1,f-1) of the weight of the vertices on the path. The determination of the paths is based on the Bellman's principle of optimality (16). The Bellman's principle of optimality states that the total length of all edges is only minimal if for each subset, the length of all edges becomes minimal as well. Let B (i,j) denote the weight of a path of minimum weight to the node $h_{i,j}$. By application of Bellman's principle of optimality the following equation can be obtained:

$$B(i,j) = l_{i,j} + \min\{B(i-1,j), B(i,j-1)\} \text{ for } i>0 \text{ or } j>0 \qquad \text{Eq. 9.}$$

$$B(0,0) = l_{0,0} \qquad \text{Eq. 10.}$$

whereat $l_{i,j}$ is the weight of the grid node $h_{i,j}$. The min-part of the equation is a direct result of the monotone path, because for a monotone path through the grid graph there are only two possibilities to chose the predecessor for grid node $h_{i,j}$: the grid nodes $h_{i-1,j}$ and $h_{i,j-1}$, and considering Bellman's principle of optimality the shorter one has to been chosen.

This formula can be evaluated by successively calculating the B(i,j) starting with B(0,0). In every step, all those B(i,j) are evaluated for which the information required on the right side of the formula is available. In the example, this first holds for B(1,0) and B(1.1). From those, B(2,0), B(1,1) and B(0,2) can be calculated. Now the information for B(2,1) and B(1,2) is available, and finally these values help to calculate B(2,2). For every node $h_{i,j}$ of the grid graph, a link is set to that one of the vertices $h_{k,l}$, (k.l) = (i-1,j) or (k,l)=(j,j-1), for which B(k,l) has achieved the minimum when evaluating B(i,j). Following the sequence of links backward from h(2,2) in the example yields the sequence of grid nodes of the minimum-weighed path from h(0,0) to h(2,2). The grid nodes of the path define the edges of an optimum triangulation (**Figure 6b**).

4.5 Calculation of the Point Pairs of the Quasi-Line of Action

In order to calculate the point pairs with the minimal distance along a triangulation edge, it must first be determined on which rotor surface the calculation shall be carried out (choice of perspective). From the numeric point of view, the determination of the perspective can have a significant influence on the calculated result, because to one point in the image area of one rotor surface there will always be determined one point on the other rotor surface with minimal distance by means of Newton iteration. In this context, the Newton iteration is the critical operation, since usually it will provide good results, if a good initial value is given and if the surface in the search area does not show strong curvatures or turnarounds. For this reason, it is advisable to carry out the Newton iteration on the rotor with the lower number of lobes and the larger radii. Alternatively, both perspectives could be used leaving the interpretation of the result to the user; this however results in a considerable increase in computation time.

Having established the amount of triangulation edges T, exactly one point of minimal distance is searched on each edge in dependence on the parameter X. With a_i and b_j being the points of an edge $t_{i,j}$ in the parameter range, the following function for the calculation of the parameters f_{ij} along the edge can be defined.

$$f_{i,j}(x) = a_i + x \cdot (b_i - a_i), 0 \le x \le 1 \qquad \text{Eq. 11.}$$

Thus, in the parameter range, this function runs linearly from a_i to b_j and reflects the parameter pair (u,v) as a result. Based on the parametric function of the NURBS-surface S, the related points $P_{x,ij}$ in the image area are calculated.

$$S(f_{i,j}(x)) = P_{x,ij}, P_{x,ij} \in R^3, \; 0 \le x \le 1 \qquad \text{Eq. 12.}$$

The Newton iteration is used for the determination of distances, with the calculation being only dependent on the parameter x. Thus, e.g. based on the Golden Ratio (16), a minimum search can be carried out in dependence of parameter x. The calculation of the bounding volume carried out at the beginning, can now be used for the generation of initial values for the Newton iteration and can thus contribute to reliable and precise solutions. This way, a point P is calculated for each edge t which approximates the point of minimal distance. If the points are connected according to the order of the edges to form a line, the result will be the intermesh clearance on the surface of rotor A (**Figure 7**). The intermesh clearance for the surface of rotor B was included in the calculation during the Newton iteration.

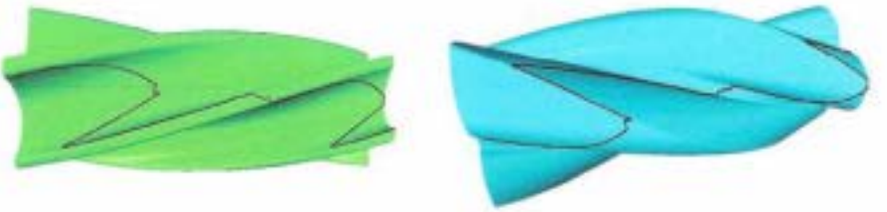

Figure 7: Intermesh clearance for female (left) and male rotor (right)

5 APPLICATION AND COMPARISON

In an application example, the intermesh clearance of a screw-type supercharger of the GL51 type is being calculated. The two rotors are given as point cloud data. At first, the B-spline areas of the rotors must be calculated. The interpolation algorithm according to (11) is used. Afterwards, a bounding volume hierarchy is calculated for each rotor. In this case, spheres are used as bounding volume

elements, since for the selected example they lead to better results than cuboids and, at the same time, they require less computation effort in the analysis. The depth of the hierarchy is 7, thus during the simultaneous depth analysis of the rotors the parameter level is divided in up to 16384 squares. This order of magnitude provides good approximation of the surfaces. The next step is the collision test. The minimum distance of the iso-distance lines is chosen in a way that as small as possible a region in the parameter range of the rotors is defined; however the region must not decompose. In this case, it turned out that a minimum distance of 0.2 mm provides a good result.

The perspective is pre-determined. Since the female rotor is the geometrically more complex rotor, the triangulation and concurrent definition of the search area is carried out in the parameter range of the female rotor. Thus the Newton iteration is carried out on the surface of the male rotor.

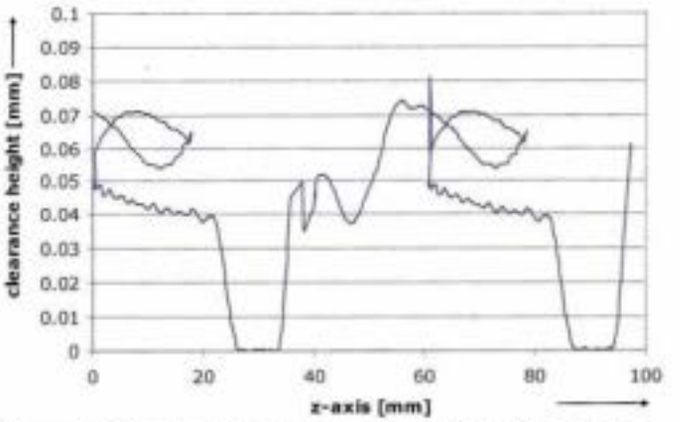

Figure 8: Gap height curve as a function of the length in rotor axis direction

In **Figure 8,** the height of the intermesh clearance along the rotor axis is shown. At first sight, the periodicity of the rotor geometry is to be seen. The characteristics of the curve repeat themselves. Furthermore, it is to be noticed that the maximal clearance height is about 0.08 mm. The collision of the two rotors at the point in which the clearance height is 0.0 mm can be explained by the fact that this machine is not synchronized. Rather does the male rotor drive the female rotor, with contact being required for power transmission.

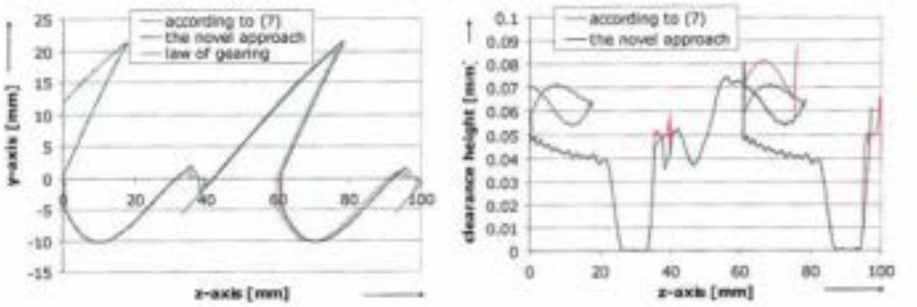

Figure 9: Projected clearance path in YZ and clearance height as a function of the Z-coordinate in comparison to (7)

The comparison of the projected clearance path and the resulting clearance heights with the results calculated by means of the methods presented in (7) is shown in **Figure 9**. Moreover, the geometrically calculated clearance paths are compared to the path of the contact line of the ideal profile according to the law of gearing. Here, it becomes clear that the spatial positions of the line of action and the quasi-line of action are slightly different, so that the line of action can be used for the assessment of the real clearance heights only with the respective loss of accuracy.

The comparison of the clearance heights with the method according to (7) shows that to a large extent, both methods provide almost identical clearance heights; however there are deviations in two areas. One deviation concerns the imaging of undercuts towards the z-coordinate. The undercut at the beginning of the rotor pair (z=0mm) is not calculated by the method according to (7) and is consequently missing in the clearance path. This is due to the generation of the initial quasi-line of action, since this is a priori situated between two points of minimal distance determined in the transverse section, and thus an undercut at the beginning or the end of the rotor surface is excluded. Furthermore, there are differences noticeable in the area of the blowhole at the pressure side (60mm<z<80mm). Here, the quasi-line of action calculated by the new method follows the line of contact of the ideal profile pair, with the consequence that in contrast to the method according to (7), a smaller distance is calculated in this area. Since the quasi-line of action has been defined as the line of the minimum distance at the start, the result of the new approach can be regarded as an improvement.

In addition, the method bears the advantage of being flexibly applicable to all parametric areas and thus e.g. also to the calculation of the housing gaps. A specific further development can improve stability and numeric efficiency of the method. Here, e.g. the generally applicable treatment of several iso-distance lines is a decisive factor.

REFERENCE LIST

(1) Niemann G., Winter, H.: Maschinenelemente Band II, Zahnradgetriebe-Grundlagen, Springer Verlag Berlin, Heidelberg 1989

(2) Schüler, R.: Entwicklung von Schraubenmaschinen-Rotoren - Ein Beitrag zur Optimierung von Schraubenmaschinen, Dissertation, Universität Dortmund, 1984

(3) Zaytsev, D, Infante Ferreira, C.A.: Profile generation method for twin screw compressor rotors based on the meshing line, International Journal of Refrigeration, Volume 28, Issue 5, pp. 744-755, 2005.

(4) Yu-Ren, W, Fong, Z.: Improved rotor profiling based on the arbitrary sealing line for twin-screw compressors, Mechanism and Machine Theory, Volume 43, Issue 6, pp. 695-711, 2008.

(5) Kauder, K, Rau, B.: Ein Verfahren zur Bestimmung der Rotoreingriffsgeometrie bei Schraubenmaschinenrotoren, Schraubenmaschinen, Nr. 1, Seite 18-24, Dortmund, 1993

(6) Huang, Y. et. al: Two-dimensional localisation and clearance evaluation of screw rotors, International Journal of Computer Applications in Technology, Volume 37, Number 1, pp. 74-85, 2010

(7) Janicki, M.: Ein Programm zur Profileingriffsspaltberechnung von verformten Schraubenmaschinen, Nr. 4, Seite 108-112, Dortmund, 1996

(8) Piegl, Les A. Tiller, W.: The NURBS Book (Monographs in Visual Communication), 2nd printing, Springer, 1996

(9) Temming, J.: Stationärer und instationärer Betrieb eines unsynchronisierten Schraubenladers. Dissertation, Universität Dortmund, 2007

(10) Ma, W., Kruth, J.P.: NURBS curve and surface fitting for reverse engineering. In: The International Journal of Advanced Manufacturing Technology 14, Volume 12, pp. 918-927, 1998
(11) Weinert, Mehnen: Discrete NURBS-Surface Approximation using an Evolutionary Strategy, Tech. Rep. Department of Machining Technology, University of Dortmund, Germany, 2000.
(12) Ericson, C.: Real-time collision detection. Morgan Kaufmann, 2005
(13) Lorensen, William E., Cline, H.: Marching cubes: A high resolution 3D surface construction algorithm, Computer Graphics, Volume 21, Number 4, pp. 163-169, 1987
(14) Fuchs, H., Kedem, Z., Uselton, S.: Optimal Surface Reconstruction from Planar Contours. Communications of the ACM, Volume 20, Number 10, pp. 693-702, 1977
(15) Bellman, R. E.: Dynamic Programming, Princeton, Princeton University Press, 1957
(16) Press,W., Flannery, B., Teukolsky, S., Vetterling,W.: Numerical Recipes in C: The Art of Scientific Computing, Cambridge University Press, 1992

Improvement of volumetric efficiency for screw compressors using inertial charging

H Kameya
Ishinomaki Senshu University, Japan
M Ishikawa
Hitachi Research Laboratory, Hitachi, Ltd., Japan
T Saito
Social Infrastructure & Industrial Machinery Systems Group,
Hitachi Plant Technologies, Ltd., Japan

ABSTRACT

Suction air flow in an oil-free screw compressor is so fast that it can be applied for improving volumetric efficiency. Such efficiency greatly depends on the close timing of a suction port. We investigated the most appropriate timing by using computational fluid dynamics and experimentally verified increased efficiency by this timing on a compressor model. Appropriate close timing is 30 degrees behind on a male rotor rotation from the moment when a working chamber is at maximum volume. This timing increases volumetric efficiency by 1.5% compared to the conventional model in which the suction port closes 15 degrees behind.

1 INTRODUCTION

Improving efficiency of a screw compressor is an important issue and has been studied at many universities, companies, and institutions with diverse mechanical engineering expertise. Since a screw compressor is a kind of positive displacement compressor, the knowledge base tends to be based on geometry rather than fluid dynamics [1]. We improved volumetric efficiency using the inertia of suction charging as an application of fluid dynamics.

An appropriate close timing of a suction port is thought to improve volumetric efficiency. The timing should be synchronized with the moment at which a working chamber's volume is at maximum when inertia of air flow is ignored. The actual appropriate close timing may be delayed due to air flow inertia. However, it is difficult to define the exact delay because of air compressibility and the three-dimensional distributions of air pressure and velocity.

Therefore, we use computational fluid dynamics (CFD) technology, in which remarkable progress has been made over the past decade [2]. We investigated the most appropriate close timing by using CFD on a model of an oil-free screw compressor and quantitatively verified this timing with an experiment.

2 COMPRESSOR STRUCTURE

The structure of an oil-free screw compressor is shown in Fig. 1, and its specifications are listed in Table 1. This compressor has male and female rotors,